Body temperatures of modern and extinct vertebrates from ^{13}C-^{18}O bond abundances in bioapatite

Robert A. Eagle[a,1], Edwin A. Schauble[b], Aradhna K. Tripati[a,b,c], Thomas Tütken[d], Richard C. Hulbert[e], and John M. Eiler[a]

[a]Division of Geological and Planetary Sciences, California Institute of Technology, Pasadena, CA 91125; [b]Department of Earth and Space Sciences, University of California, Los Angeles, CA 90095; [c]Department of Earth Sciences, University of Cambridge, Downing Street, Cambridge, CB2 3EQ, United Kingdom; [d]Steinmann-Institut für Geologie Mineralogie und Paläontologie, Universität Bonn, Poppelsdorfer Schloss, 53115 Bonn, Germany; and [e]Florida Museum of Natural History, University of Florida, Gainesville, FL 32611

Edited by Mark H. Thiemens, University of California, San Diego, La Jolla, CA, and approved April 16, 2010 (received for review October 1, 2009)

The stable isotope compositions of biologically precipitated apatite in bone, teeth, and scales are widely used to obtain information on the diet, behavior, and physiology of extinct organisms and to reconstruct past climate. Here we report the application of a new type of geochemical measurement to bioapatite, a "clumped-isotope" paleothermometer, based on the thermodynamically driven preference for ^{13}C and ^{18}O to bond with each other within carbonate ions in the bioapatite crystal lattice. This effect is dependent on temperature but, unlike conventional stable isotope paleothermometers, is independent from the isotopic composition of water from which the mineral formed. We show that the abundance of ^{13}C-^{18}O bonds in the carbonate component of tooth bioapatite from modern specimens decreases with increasing body temperature of the animal, following a relationship between isotope "clumping" and temperature that is statistically indistinguishable from inorganic calcite. This result is in agreement with a theoretical model of isotopic ordering in carbonate ion groups in apatite and calcite. This thermometer constrains body temperatures of bioapatite-producing organisms with an accuracy of 1–2 °C. Analyses of fossilized tooth enamel of both Pleistocene and Miocene age yielded temperatures within error of those derived from similar modern taxa. Clumped-isotope analysis of bioapatite represents a new approach in the study of the thermophysiology of extinct species, allowing the first direct measurement of their body temperatures. It will also open new avenues in the study of paleoclimate, as the measurement of clumped isotopes in phosphorites and fossils has the potential to reconstruct environmental temperatures.

apatite | isotope | paleoclimate | thermophysiology | paleothermometry

The mechanisms by which animals regulate their body temperatures are among the most fundamental aspects of their biology. The acquisition of endothermy, the ability to maintain high and stable body temperatures through internal heat production, is a major physiological change that occurred at an unknown stage during the evolutionary transition to mammals and birds from their ancestors among the nonmammalian therapsids and nonavian dinosaurs, respectively (1). Approaches to understanding the physiology of extinct animals and the evolution of endothermy have largely focused on biophysical modeling, anatomical observations, growth rate analysis from bone histology, and behavioral studies such as estimating predator/prey ratios (1–7). The validity of each of these approaches is uncertain (for contrasting viewpoints on approaches to dinosaur thermoregulation see refs. 4 and 5).

Modern endothermic mammals and ectotherms, such as alligators and crocodiles, generally have significant differences in average body temperatures. With rare exceptions, mammals have high and stable body temperatures around 36–38 °C regardless of their environment, whereas the body temperatures of ectotherms are generally lower on average and often fluctuate depending on environmental temperatures (1). While not a completely unambiguous indicator of physiology, the ability to measure the body temperature of extinct vertebrates would provide crucial information in tracing the evolution of thermoregulation. However it has been widely assumed that it would not be possible to make a direct measurement of the body temperatures of extinct organisms (2, 8).

An indirect geochemical approach to reconstructing temperature is based on the oxygen isotope composition ($\delta^{18}O$) of minerals such as calcite, aragonite, and apatite (9–12). However, the $\delta^{18}O$ values of these minerals depend on both growth temperature and the $\delta^{18}O$ of the water from which the mineral formed. Because waters are rarely preserved in the geologic record, it is generally necessary to assume a value for the $\delta^{18}O$ of water in order to draw conclusions regarding biomineral growth temperatures.

The oxygen isotope composition ($\delta^{18}O$) of the phosphate and carbonate component of bioapatite in bone, teeth, and scales reflects both the body temperature of the animal and the oxygen isotope composition of its body fluids (13–19). The $\delta^{18}O$ of body waters, and hence bioapatite, can be influenced by local meteoric water compositions (14, 15, 19, 20), humidity (20–23), diet (24, 25), and physiology of the animal (19, 20, 24, 25). The complex factors influencing body water $\delta^{18}O$ mean that it is difficult to make robust assumptions regarding the body water $\delta^{18}O$ of an extinct species. Attempts have been made to address thermoregulation in extinct species with the oxygen isotope thermometer. However, these studies are to some extent ambiguous due to the requirement for assumptions regarding body water $\delta^{18}O$ (26–28) and the preservation of primary oxygen isotope compositions when fossil bone was analyzed (29, 30).

Here we describe the application of a previously undescribed approach to bioapatite—the carbonate "clumped-isotope" thermometer—that holds promise for overcoming some of the drawbacks of oxygen isotope paleothermometry and providing a relatively assumption-free measurement of body temperatures of extinct species. Clumped-isotope thermometry relies on the propensity of ^{13}C and ^{18}O to form bonds, or "clump," with each other in a carbonate molecule. This effect is independent of bulk isotopic compositions but is dependent on temperature (31–33). The abundance of ^{13}C-^{18}O bonds in carbonate can be determined from the abundance of mass 47 CO_2 produced on phosphoric acid digestion of carbonate-containing minerals. The relationship between temperature and ^{13}C-^{18}O bond abundance is defined by the deviation of the measured abundance of mass 47 CO_2 compared to the abundance of mass 47 CO_2 expected for a random distribution of isotopes and is given the notation Δ_{47} (34). As $\delta^{13}C$

Author contributions: R.A.E., E.A.S., and J.M.E. designed research; R.A.E. and E.A.S. performed research; R.A.E., E.A.S., A.K.T., and J.M.E. analyzed data; T.T. and R.C.H. contributed new reagents/analytic tools; and R.A.E. and E.A.S. wrote the paper.

The authors declare no conflict of interest.

This article is a PNAS Direct Submission.

[1]To whom correspondence should be addressed. Email: robeagle@caltech.edu.

This article contains supporting information online at www.pnas.org/lookup/suppl/doi:10.1073/pnas.0911115107/-/DCSupplemental.

and $\delta^{18}O$ are simultaneously determined, this approach also allows an assumption-free calculation of the $\delta^{18}O$ of the water from which the mineral formed. Carbonate clumped-isotope thermometry has been applied to a number of materials and questions, including using soil carbonates to examine the uplift history of the Altiplano (35), brachiopods to examine Phanerozoic marine temperatures (36), and speleothems to examine glacial-interglacial terrestrial climate change (37)

Results and Discussion

Clumped-Isotope Analysis of Modern Bioapatite. Ghosh et al. (31) derived the following relationship between the Δ_{47} value of CO_2 extracted from inorganic calcite grown at temperatures ranging from 0–50 °C, on reaction with phosphoric acid at 25 °C:

$$\Delta_{47} = 0.0592 \times 10^6 \times T^{-2} - 0.02 \quad [1]$$

In order to assess the relationship between growth temperature and the Δ_{47} value of CO_2 extracted from bioapatite, we made measurements on a range of modern vertebrate species whose physiologies are well constrained (Table 1).

Samples of tooth enamel from a single tooth from a modern Indian elephant (*Elephas maximus indicus*) and a single tooth from a modern white rhinoceros (*Ceratotherium simum*) were analyzed from six and four separate CO_2 extractions, respectively. The published calibration of the carbonate clumped-isotope thermometer for inorganic calcite predicts a Δ_{47} value of 0.596‰ for calcite grown at 37 °C (31), which is the average body temperature of almost all placental mammals (31, 38). Analysis of rhinoceros and elephant tooth enamel bioapatite yielded Δ_{47} values of 0.597 ± 0.006‰ (1 s.e.) and 0.596 ± 0.008‰, respectively (Table 1). Therefore Δ_{47} measurements from mammal bioapatite are indistinguishable from values of inorganic calcite grown at equilibrium at the same temperature. See *Methods* for more details on error estimation.

In order to evaluate the temperature sensitivity of the carbonate clumped-isotope thermometer in bioapatite we also analyzed specimens from "cold-blooded" (ectothermic) vertebrates (Table 1 and Fig. 1), specifically teeth from modern Nile crocodiles (*Crocodylus niloticus*) from Egypt and modern American alligators (*Alligator mississippiensis*) from a farm in Colorado. Enamel/dentin mixtures from ectotherm teeth were analyzed because their enamel is very thin. The body temperatures of these species are known to fluctuate daily by 8–12 °C, and by as much as 20 °C during the course of a year (6, 39, 40). Therefore there is some uncertainty over exactly what body temperatures biomineralization occurs at in these species. Both Nile crocodiles and American alligators have been observed to reduce growth (i.e., to grow at low rates or not grow at all) in the cold season months,

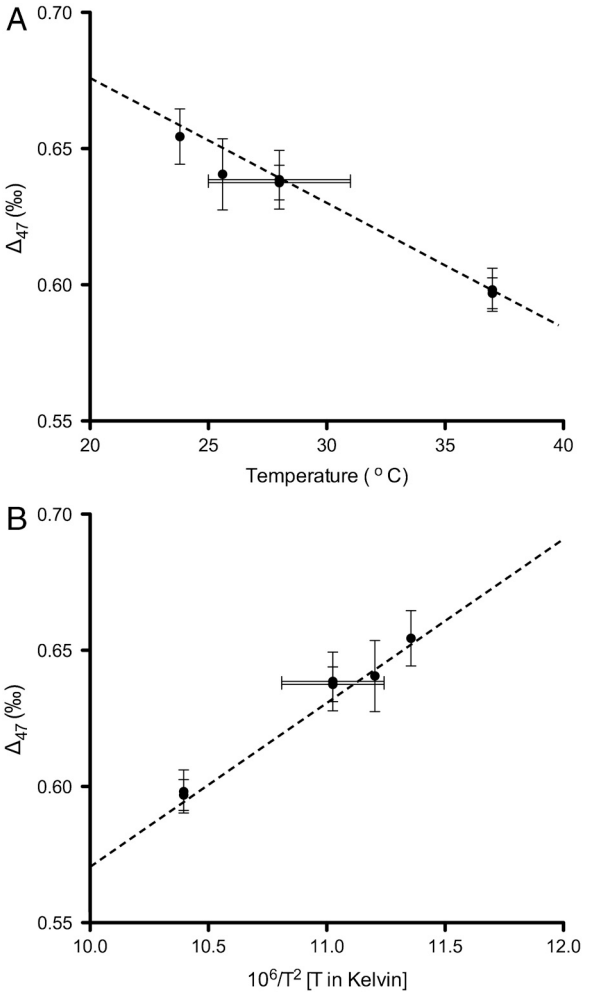

Fig. 1. The relationship between measured Δ_{47} values from bioapatite and the body temperature of the organism. The Y-value for each data point represents the mean Δ_{47} value derived from 3–7 measurements of distinct extractions of CO_2 from tooth bioapatite. Y-axis error bars represent the external precision of the measurement, to one standard error. The X-axis scale shows the predicted body temperature of each species, based on previous studies on their thermoregulation, as described in detail in the main text. X-axis error bars represent uncertainties in body temperatures. (*A*) Δ_{47} data plotted against temperature, reported in °C. (*B*) The same data plotted as $10^6/T^2$ [*T* in Kelvin]. The inorganic calcite calibration derived by Ghosh et al. is plotted as a dotted line (31). Δ_{47} measurements of CO_2 extracted from bioapatite all fall within one standard error of the inorganic calcite line.

Table 1. Δ_{47} measurements from tooth bioapatite of modern species

Species	n *	Δ_{47}	Estimated Body Temperature (°C) †	Δ_{47} Temperature (°C) ‡
White Rhinoceros (*Ceratotherium simum*)	6	0.597 ± 0.006	37	36.6 ± 1.4
Indian Elephant (*Elephas maximus indicus*)	4	0.596 ± 0.008	37	36.9 ± 2.0
Nile Crocodile (*Crocodylus niloticus*)	7	0.638 ± 0.006	28 ± 3	26.9 ± 1.4
American Alligator (*Alligator mississippiensis*)	3	0.639 ± 0.011	28 ± 3	26.7 ± 2.5
Sand Tiger Shark (*Carcharias taurus*)	5	0.641 ± 0.013	25.3	26.2 ± 3.0
Sand Tiger Shark (*Carcharias taurus*)	3	0.654 ± 0.010	23.6	23.1 ± 2.3

± Uncertainty in Δ_{47} values represent the external precision of the measurement (one standard error). Uncertainty in Δ_{47} body temperature values represent the error in body temperatures in °C propagated from the external precision of the Δ_{47} measurement (one standard error).

*Number of distinct extractions of CO_2 from bioapatite analyzed for each species. Between 1–5 teeth for each species were analyzed. Data for individual extractions is shown in Table S1.

†Estimated from published body temperature measurements (see main text for details). In the case of sand tiger sharks the two samples were from two different aquariums with different ambient water temperatures.

‡Calculated assuming Δ_{47} values in bioapatite exhibit the same temperature dependency as inorganic calcite, given in Eq. **1**.

which has been attributed to a reduction in food intake and in some instances, hibernation (41, 42). Based on published studies on alligator and crocodile thermoregulation we estimated an average spring-to-autumn body temperature of 28 °C for a medium sized adult, with an uncertainty of ±3 °C (6, 39, 40). The low temperature points on our calibration were from the analysis of enamel/dentin mixtures from Sand Tiger shark (*Carcharias taurus*) teeth that were kept at distinct and stable water temperatures of 25.3 °C and 23.6 °C in two separate aquariums. Shark body temperatures were assumed to reflect ambient water temperatures (43). Individual stable isotope measurements used to calculate the average results presented in Table 1 and Fig. 1 are given in *SI Text*.

All bioapatite data are within one standard error of the inorganic calcite calibration line (Fig. 1 and Eq. **1**) of Ghosh et al. (31). Eq. **1** represents a line of best fit through the Δ_{47} values for inorganic calcite and uses arithmetic means calculated from data for multiple extractions (31). Huntington et al. (44) performed a weighted least squares linear regression on inorganic calcite calibration data from Ghosh et al. (31) to take into account both the error in each measurement and the uncertainty in the absolute growth temperature of each synthetic calcite. This regression was carried out using the weighted mean Δ_{47} value for each sample. The algorithm of York was used for this analysis (45). This analysis yielded the following relationship:

$$\Delta_{47} = (0.0605 \pm 0.0014) \times 10^6 \times T^{-2} - (0.031 \pm 0.016) \quad \textbf{[2]}$$

We carried out the same regression analysis for the inorganic calcite data from Ghosh et al. (31) using arithmetic means, which results in:

$$\Delta_{47} = (0.0588 \pm 0.0046) \times 10^6 \times T^{-2} - (0.014 \pm 0.047) \quad \textbf{[3]}$$

We also applied this regression model to arithmetic mean values for the bioapatite data using taxon mean Δ_{47} values (Fig. 1 and Table 1) and get the following result:

$$\Delta_{47} = (0.0594 \pm 0.0096) \times 10^6 \times T^{-2} - (0.021 \pm 0.103) \quad \textbf{[4]}$$

A Student's T-test shows that the slope and intercept of the calcite and apatite calibrations (Eqs **3** and **4**) are statistically indistinguishable from each other (for the slope, $p = 0.8962$; for the intercept, $p = 0.8886$). For the population of modern apatite samples ($n = 6$), the root mean square error (RMSE) of the residuals (between Δ_{47} values predicted from the inorganic calcite calibration and measured Δ_{47} of CO_2 extracted from apatite) is 0.004‰. The RSME is a standard measure of how close a fitted line is to data points (i.e., the goodness of fit) and reports the average distance (measured along a vertical line) between each data point from the regression. It is interpretable in measurement units; in this case, the RMSE is less than the external precision of Δ_{47} measurements in the bioapatite calibration (1 s.e.; see *Methods* for a more detailed description of the treatment of errors).

In theoretical models, it has been shown that in a variety of carbonate minerals (calcite, aragonite, dolomite, magnesite, witherite, and nahcolite) the crystal structure and the identity of the cation has only a modest influence of the abundance of ^{13}C-^{18}O bonds (32). Shark tooth enameloid mainly consists of fluorapatite, rather than hydroxyapatite that predominates in mammalian teeth (46). Because measurements on both types of apatite are within one standard error of the inorganic calcite calibration lines (Fig. 1), this further reinforces the conclusion that mineral structure and composition only have a minor influence on the abundance of ^{13}C-^{18}O bonds in the carbonate component. It also suggests that the isotopic fractionation associated with phosphoric acid digestion of apatite must be similar to that of calcite (47).

These data are consistent with the hypothesis that the ordering of ^{13}C-^{18}O bonds in carbonate minerals records the state of ordering of bonds in the dissolved inorganic carbon (DIC) pool (i.e., HCO_3^- and CO_3^{2-} ions) from which bioapatite grows, which are in isotopic equilibrium with body water (48–50). Studies of other calcifying organisms also support this hypothesis; for example, it has been shown that Δ_{47} measurements of both calcitic and aragonitic foraminifera and corals are at equilibrium, whereas both are well known to show nonequilibrium $\delta^{18}O$ and $\delta^{13}C$ values (31, 49, 50).

Thermodynamic Model of Clumped-Isotope Equilibrium in Apatite. We further investigated the relationship between growth temperature and the Δ_{47} values of CO_2 extracted from bioapatite by creating a theoretical thermodynamic model describing the equilibrium constant for isotopic order–disorder reactions in carbonate ion units in crystalline apatite. This model is based on "B-type" carbonate substitution into apatite—where a CO_3^{2-} group replaces one PO_4^{3-} group in each unit cell. B-type substitution is thought to be the dominant mechanism for incorporating carbonate into the apatite structure (51). This model is based on first-principles descriptions of force constants on bonds within carbonate-apatite and a statistical-thermodynamic treatment of equilibrium constants for relevant isotope exchange reactions. Fluorapatite is chosen because it has a simpler unit cell than hydroxylapatite, facilitating density-functional theory calculations. Further details of the model are given in *SI Text*.

Calculated ^{13}C-^{18}O clumping equilibria (K_{eq}) are shown in Fig. 2. Results for a calcite model constructed with the same pseudopotentials and energy cutoff parameters are also given. See Schauble et al. (32) for a more general treatment of such models in solid carbonates. The positionally averaged K_{eq} of B-type carbonate-substituted fluorapatite is remarkably similar to the analogous calcite model as well as to a previously described calcite model created with different software and pseudopotentials (29). Differences among the three models are equivalent to 1–2 °C at a given Δ_{47} value of CO_2. Thus, barring systematic differences in Δ_{47} arising from variations in the acid-digestion fractionation (47), these models predict that the carbonate clumped-isotope thermometer for carbonate apatite should be nearly indistinguishable from that for calcite. We consider this to be a relatively simplified and preliminary theoretical calculation because it will be necessary to construct models that permit various alternative substitutions in both fluorapatite and hydroxylapatite. Nevertheless, this model result provides a context for understanding our empirical observation that the calcite and apatite calibrations are indistinguishable.

Considering both the empirical and theoretical results, we can draw two inferences. Firstly, as both the model and data show that K_{eq} and measured Δ_{47} values in apatite and calcite are indistinguishable, this suggests that the acid-digestion fractionation factors for apatite and calcite ($\alpha_{CO2\text{-apatite}}$ and ($\alpha_{CO2\text{-calcite}}$) are also indistinguishable within the error of our Δ_{47} measurements. Secondly, as the theoretical values of K_{eq} for the reactions governing ^{13}C-^{18}O bond abundance in calcite and apatite are almost identical, our data cannot prove the hypothesis that clumping is set in the DIC pool, although it is consistent with it.

Measuring the Body Temperatures of Extinct Species. In order the test the ability of clumped-isotope thermometry to measure the body temperature of an extinct organism from fossilized bioapatite, we made measurements from woolly mammoth (*Mammuthus primigenius*) teeth from the Late Pleistocene. The teeth examined were derived from two sites (*SI Text*): the upper Rhine River valley, where specimens were recovered by dredging gravel pits proximal to the Rhine River (52, 53); and the southern North Sea, where specimens were obtained by dredging with ground reaching fishing nets (54, 55). One specimen

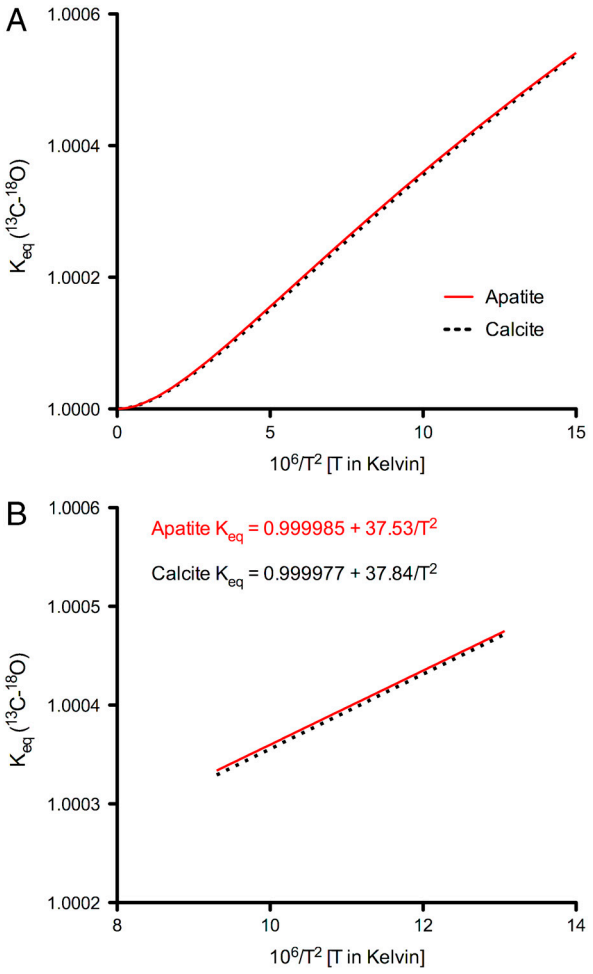

Fig. 2. *A* shows the results of first-principles theoretical calculations of the equilibrium constant for the ^{13}C-^{18}O "clumping" equilibria, plotted versus temperature, for carbonate-bearing apatite (solid red line), and calcite (dotted black line). In *B* the X-axis is $10^6/T^2$ [*T* in Kelvin] over the relevant biological temperature range (276–328 K). The modeled K_{eq} of apatite and calcite are almost identical.

from each site was selected for analysis because they were exposed to different burial environments and diagenetic fluids (freshwater and seawater). These samples are described in more detail in a previous study (56), where the oxygen isotope composition of phosphate ($\delta^{18}O_{PO4}$), the nitrogen content, and rare earth element (REE) composition were examined. Both $\delta^{18}O_{PO4}$ and REE content suggested a degree of diagenic alteration in the dentin component of the teeth but not in the enamel component (56).

Measurements of Δ_{47} in enamel from both localities were within one standard error of the measured value for a modern Indian elephant and also within error of the predicted Δ_{47} of inorganic calcite grown at 37 °C (Table 2). Combining the measurements on mammoth enamel from both sites yielded a Δ_{47} value of $0.590 \pm 0.007‰$ (1 s.e; Table 2). Solving Eq. **1** with this value yields a body temperature of 38.4 ± 1.8 °C for *Mammuthus primigenius*, an expected number based on their similarity to modern large mammals such as elephants (38).

In contrast, the dentin component of teeth from both sites yielded lower temperatures of 25.6 °C and 30.9 °C from the Rhine River and North Sea specimens respectively. These temperatures are unlikely to equal the temperatures of the diagenetic fluids that each specimen was exposed to but is consistent with partial recrystallization at lower temperatures. These data are consistent with widespread evidence that organic-rich dentin, which contains smaller apatite crystals, is more susceptible to diagenetic alteration than the large and closely packed apatite crystals found in (relatively organic-poor) enamel (17, 56, 57). None of the fossil material analyzed here showed significant alteration in X-ray diffraction peak shape, which is sometimes used as an indicator of recrystalization (58; Fig. S2).

To assess the utility of clumped-isotope thermometry in accurate determination of body temperatures for much older fossil material, we analyzed enamel from extinct Miocene rhinocerotid and alligator species. Specimens are from the Agricola Road Site in Polk County, Florida. The age of the deposit is late middle Miocene, *ca.* 12 Ma, based on a biochronologic assessment of the diverse assemblage of equids (59, 60). Measurements from Miocene rhinoceroses and alligators were within error of modern mammals and alligators, respectively (Table 3). A 6 °C difference between endotherm and ectotherm body temperature was resolved. Therefore clumped-isotope thermometry has the potential to accurately reconstruct body temperatures and resolve different thermophysiologies from fossil teeth of at least Miocene age.

Conclusions

Previous attempts to address the body temperatures of extinct species using stable isotope geochemistry have been limited by the assumptions necessary to apply the traditional oxygen isotope thermometer (23, 25). Here we have shown that by analyzing ^{13}C-^{18}O bonds in the carbonate component of bioapatite it is possible to make robust and relatively assumption-free measurements of the body temperatures of extinct species using enamel from teeth that are millions of years old. An external precision of 0.005–0.010‰ was routinely achievable in this study, showing that it should be possible to reconstruct body temperatures from fossil teeth with an error of 1–2 °C. Application of this technique to well-preserved bioapatite from more ancient extinct species (e.g., nonavian dinosaurs) offers a previously undescribed approach to study the evolution of thermoregulation. The clumped-isotope analysis of the carbonate component of phosphate minerals also has considerable potential in other areas.

Table 2. Δ_{47} measurements from fossil mammoth tooth bioapatite

Sample	Locality	n *	Δ_{47}	Δ_{47} Temperature (°C)
Enamel	Rhine River	4	0.587 ± 0.011	39.1 ± 2.8
Dentin	Rhine River	3	0.643 ± 0.027	25.6 ± 6.3
Enamel	North Sea	2	0.596 ± 0.006	36.8 ± 1.3
Dentin	North Sea	2	0.620 ± 0.001	30.9 ± 0.3
Enamel	Average from both sites	6	0.590 ± 0.007	38.4 ± 1.8

± Uncertainty in Δ_{47} values represent the external precision of the measurement (one standard error if more than two analyses were made; if fewer were made, then the standard deviation is shown). Uncertainty in Δ_{47} body temperature values represent the error in body temperatures in °C propagated from the external precision of the Δ_{47} measurement (one standard error).

*Number of distinct extractions of CO_2 made from bioapatite of each species. Data for individual extractions is shown in Table S2.

Table 3. Δ_{47} measurements from Miocene mammal and ectotherm tooth bioapatite

Species	N *	Δ_{47}	Δ_{47} Body Temperature (°C) †
Rhinocerotidae Acquisitions from 2 teeth	6	0.597 ± 0.005	36.6 ± 1.3
Alligator sp. Acquisitions from 5 teeth	2	0.623 ± 0.017	30.4 ± 3.9

$\pm\Delta_{47}$, ± values represent the external precision of the measurement (one standard error if more than two analyses were made; if fewer were made, then the standard deviation is shown). Body temperature ± values represent the error in body temperatures in °C calculated by propagating the uncertainty in Δ_{47}.

*Number of distinct extractions of CO_2 made on bioapatite of each taxon. In the case of the rhinocerotid specimens, three extractions were made of each tooth. In the case of the *Alligator* sp. one extraction was made on powder from two teeth, and a second extraction on three teeth. Material from multiple alligator teeth was pooled as a necessity to gain enough enamel for analysis. Data for individual extractions is given in Table S3.

†Calculated assuming Δ_{47} values in bioapatite show the same temperature dependency as inorganic calcite, given in Eq. **1**

Oxygen isotope analysis of calcium-phosphate biomineralizing organisms such as conodonts, fish, and brachiopods are widely used in paleoclimate studies, particularly in the study of pre-Cenozoic environments. Even in materials that are subject to rapid alteration, such as bone, the isotopic composition of bioapatite may yield information on climate change by recording an early diagenetic environmental signal (61). In addition, phosphorite (carbonate fluorapatite) is found both in modern sediments and sedimentary rocks dating back to the Pre-Cambrian, and phosphorite geochemistry is widely used to obtain information on ancient marine environments (62). Therefore this study also provides a basis for the application of clumped-isotope thermometry on carbonate-containing apatite to paleoclimate questions.

Methods

Sample Preparation. Bioapatite is commonly intimately intergrown with organic matter that is a potential source of contamination to mass-47 CO_2 measurements. In order to probe the necessity of oxidative cleaning to remove organic material from apatites, a series of tests were run on samples of rhinoceros enamel. Powdered samples were either untreated or treated with aqueous solutions of 3% H_2O_2 for 15 min, 4 h, or 24 h. All treatments yielded Δ_{47} measurements that were within two standard errors of the expected value for inorganic calcite grown at 37 °C (the body temperature of a rhinoceros), except for the untreated sample (*SI Text*). Because we anticipated many samples could contain higher levels of organic matter than the enamel samples used as a test, we utilized a midrange cleaning condition in all further analyses (4 h in 3% H_2O_2). It is also common to treat fossil bioapatite samples with an acid wash to achieve selective dissolution of labile and diagenetic carbonates but not carbonate ion that is a structural component of bioapatite (58). We subjected modern elephant and Rhine River mammoth enamel and dentin to a second treatment step of 0.1 M acetic acid, buffered to pH 2.8 or pH 4.6 (*SI Text*). The Δ_{47} of mammoth dentin was much more susceptible to acid treatment than other materials, a probable indication of the presence of diagenetic carbonates (*SI Text*). Because treatments of 4 h and 24 h in pH 4.6 buffered 0.1 M acetic acid gave values within one standard error of each other, these treatments were compiled together in the construction of Table 2 (*SI Text*). The modern bioapatite calibration samples were treated for 4 h in 3% H_2O_2 but not subjected to an acid wash.

Phosphoric Acid Digestion and Mass Spectrometry. CO_2 analyte was obtained by reacting bioapatite samples in H_3PO_4 on a custom-built automated online vacuum system that is described elsewhere (Passey et al., manuscript in preparation) adapted with a large reaction vessel to allow complete acid digestion of large bioapatite samples. Because carbonate is a minor (2–10%) component of bioapatite it was necessary to react 100–200 mg of each sample to liberate enough CO_2 for analysis. Reactions were carried out at 90 °C for 20 min, and CO_2 was immediately trapped on liquid nitrogen as it evolved. Each sample was then subjected to cryogenic purification in dry ice/ethanol and liquid nitrogen traps and purification on a gas chromatograph to remove hydrocarbon contaminants according to the scheme outlined in Ghosh et al. (31). CO_2 was also passed through an Ag adsorbent to remove any sulfur gas contamination. Sample gases were analyzed for masses 44–49 on a Thermo-Finnigan MAT 253 gas source isotope ratio mass spectrometer for 8 acquisitions of 10 cycles, each with an integration time of 8 s and a total analysis time of approximately 3 h. Measurements were made with a stable 16-volt signal at mass 44, with peak centering, background measurement, and pressure-balancing before each acquisition. Detailed descriptions on the methods involved in making precise and accurate clumped-isotope measurements are given elsewhere (44).

Standardization. The majority of data for this study was collected between December 2008 and May 2009. Analyses of Miocene samples were conducted from January 3 to 7, 2010. Each day, gases that had been heated to 1,000 °C and quenched were analyzed to define the stochastic distribution of isotopologues (34). Carbonate standards were run every 4–6 analyses. Seven distinct extractions of NBS-19 reference standard during this period yielded a mean Δ_{47} value of 0.361 ± 0.008‰, $\delta^{13}C$ of 1.94 ± 0.04‰ (PDB), and a $\delta^{18}O$ of −2.2 ± 0.05‰ (PDB). Seven separate extractions of a vein calcite, termed 102-GC-AZ01, yielded a Δ_{47} of 0.646 ± 0.009‰, $\delta^{13}C$ of 0.62 ± 0.06‰ (PDB), and $\delta^{18}O$ of −13.76 ± 0.05‰ (PDB). Accepted Δ_{47} values for these standards from >40 analyses by multiple analysts in our laboratory are 0.352‰ and 0.657‰ for NBS-19 and 102-GC-AZ01 respectively.

Treatment of Errors. The error in Δ_{47} of CO_2 extracted once ('$n = 1$') from a bioapatite sample ranged from 0.006 to 0.017‰ and averaged 0.010‰. This uncertainty is calculated as one standard error of the mean Δ_{47} value determined from eight acquisitions of the same gas. The external precision for modern bioapatite samples that were analyzed multiple times ($n > 1$) ranged from 0.006 to 0.013‰ and averaged 0.009 ‰. For $n \geq 3$, this uncertainty is calculated as one standard error of the mean Δ_{47} value determined from multiple CO_2 samples extracted from separate aliquots of the same material, with each extraction analyzed for eight acquisitions. For $n = 2$, the standard deviation is reported. Huntington et al., (2009) present a more detailed description of methods and limitations of clumped-isotope thermometry (44).

For the results presented in this section, the external precision of the data is reported. The internal precision of individual stable isotope measurements is presented in SI tables. In some cases, measurements were excluded due to known or suspected errors in sample preparation and analysis. For example, in some cases incomplete acid digestions of apatite samples was observed, or too little CO_2 was derived from acid digestion to allow for stable gas pressures (i.e., 8 acquisitions at a mass 44 signal of 16 V).

ACKNOWLEDGMENTS. We would like to thank John Harris and Jim Dines at the Natural History Museum of Los Angeles County and Rob Asher and Matt Lowe at the University Museum of Zoology, Cambridge, for the provision of modern terrestrial vertebrate teeth. Also thanks to Paul Hale at the London Aquarium and Anna George at the Tennessee Aquarium Research Institute for provision of shark teeth, to Ben Passey for discussing adaptations to the automated CO_2 purification system, and to Sierra Petersen for help preparing samples. Kate Huntington generously provided MATLAB scripts for regression analysis. This work was funded through a Caltech Chancellors Postdoctoral Scholarship to R.A.E. and National Science Foundation Grants EAR-0843294 and EAR-0643394 to J.M.E.

1. Ruben J (1995) The evolution of endothermy in mammals and birds—From physiology to fossils. *Annu Rev Physiol* 57:69–95.
2. Farlow JO (1990) Dinosaur Energetics and Thermal Biology. *The Dinosauria*, eds DB Weishampel, P Dodson, and H Osmólska (University of California Press, Berkeley), 1st Ed, pp 43–55.
3. Kemp TS (2006) The origin of mammalian endothermy: a paradigm for the evolution of complex biological structure. *Zool J Linn Soc-Lond* 147:473–488.
4. Chinsamy A, Hillenius WJ (2004) Physiology of Nonavian Dinosaurs. *The Dinosauria*, eds DB Weishampel, P Dodson, and H Osmólska (University of California Press, Berkeley), 2nd Ed, pp 643–659.

5. Padian K, Horner JR (2004) Dinosaur physiology. *The Dinosauria*, eds DB Weishampel, P Dodson, and H Osmólska (University of California Press, Berkeley), 2nd Ed, pp 660–671.
6. Seebacher F, Grigg GC, Beard LA (1999) Crocodiles as dinosaurs: Behavioural thermoregulation in very large ectotherms leads to high and stable body temperatures. *J Exp Biol* 202:77–86.
7. Gillooly JF, Allen AP, Charnov EL (2006) Dinosaur fossils predict body temperatures. *PLoS Biol* 4(8):e248.
8. Terblanche JS (2007) Big dinosaurs: Hot or not? *J Exp Biol* 210(1):vi.
9. Urey HC (1947) The thermodynamic properties of isotopic substances. *J Chem Soc* 562–581.
10. McCrea JM (1950) On the isotopic chemistry of carbonates and a paleotemperature scale. *J Chem Phys* 18:849–857.
11. Epstein S, Buchsbaum R, Lowenstam H, Urey HC (1953) Revised carbonate water isotopic temperature scale. *Bull Geol Soc Am* 64:1315–1326.
12. Longinelli A, Nuti S (1973) Revised phosphate-water isotopic temperature scale. *Earth Planet Sci Lett* 19:373–376.
13. Land LS, Lundelius EL, Jr, Valastro S, Jr (1980) Isotope ecology of deer bones. *Palaeogeogr Palaeoclimatol Palaeoecol* 32:143–151.
14. Longinelli A (1984) Oxygen isotopes in mammal bone phosphate: A new tool for paleohydrological and paleoclimatological research? *Geochim Cosmochim Acta* 48:385–390.
15. Luz B, Kolodny Y (1985) Oxygen isotope variations in phosphate of biogenic apatites, IV. Mammal teeth and bones. *Earth Planet Sci Lett* 75(1):29–36.
16. Koch PL, Fischer DC, Dettman DL (1989) Oxygen isotopic variation in the tusks of extinct proboscideans; A measure of season of death and seasonality. *Geology* 17:515–519.
17. Kohn MJ, Cerling TE (2002) Stable isotope compositions of biological apatite. *Reviews in Mineralogy and Geochemistry. Phosphates: Geochemical, Geobiological, and Materials Importance*, eds MJ Kohn, J Rakovan, and JM Hughes (Mineralogical Society of America and Geochemical Society, Washington, DC), Vol 48, pp 455–488.
18. Barrick RE, Fischer AG, Showers WJ (1999) Oxygen isotopes from turtle bone: Applications for terrestrial paleoclimates? *Palaios* 14:186–191.
19. Amiot R, et al. (2007) Oxygen isotope fractionation between crocodilian phosphate and water. *Palaeogeogr Palaeoclimatol Palaeoecol* 243:412–420.
20. Levin NE, Cerling TE, Passey BH, Harris JM, Ehleringer JR (2006) A stable isotope aridity index for terrestrial environments. *Proc Natl Acad Sci USA* 103(30):11201–11205.
21. Ayliffe LK, Chivas AR (1990) Oxygen isotope composition of bone phosphate of Australian kangaroos: Potential as a palaeoenvironmental recorder. *Geochim Cosmochim Acta* 54:2603–2609.
22. Luz B, Cormie AB, Schwarcz HP (1990) Oxygen isotope variations in phosphate of deer bones. *Geochim Cosmochim Acta* 54:1723–1728.
23. Cormie AB, Luz B, Schwarcz HP (1994) Relationship between the hydrogen and oxygen isotopes of deer bone and their use in the estimation of relative humidity. *Geochim Cosmochim Acta* 58(16):3439–3449.
24. Kohn MJ (1996) Predicting animal $\delta^{18}O$: Accounting for diet and physiological adaptation. *Geochim Cosmochim Acta* 60(23):4811–4819.
25. Kohn MJ, Schoeninger MJ, Valley JW (1996) Herbivore tooth oxygen isotope compositions: Effects of diet and physiology. *Geochim Cosmochim Acta* 60(20):3889–3896.
26. Fricke HC, Rogers RR (2000) Multiple taxon-multiple locality approach to providing oxygen isotope evidence for warm-blooded theropod dinosaurs. *Geology* 28 (9):799–802.
27. Barrick RE, Kohn MJ (2001) Comment: Multiple taxon-multiple locality approach to providing oxygen isotope evidence for warm-blooded theropod dinosaurs. *Geology* 29(6):565–566.
28. Amiot R, et al. (2006) Oxygen isotopes from biogenic apatites suggest widespread endothermy in Cretaceous dinosaurs. *Earth Planet Sci Lett* 246(1-2):41–54.
29. Barrick RE, Showers WJ (1994) Thermophysiology of *Tyrannosaurus rex*: Evidence from oxygen isotopes. *Science* 265(5169):222–224.
30. Kolodny Y, Luz B, Sander M, Clemens WA (1996) Dinosaur bones: Fossils or pseudomorphs? The pitfalls of physiology reconstruction from apatitic fossils. *Palaeogeogr Palaeoclimatol Palaeoecol* 126:161–171.
31. Ghosh P, et al. (2006) ^{13}C-^{18}O bonds in carbonate minerals: A new kind of paleothermometer. *Geochim Cosmochim Acta* 70(6):1439–1456.
32. Schauble EA, Ghosh P, Eiler JM (2006) Preferential formation of ^{13}C-^{18}O bonds in carbonate minerals, estimated using first-principles lattice dynamics. *Geochim Cosmochim Acta* 70(10):2510–2529.
33. Eiler JM (2007) "Clumped-isotope" geochemistry—The study of naturally-occurring, multiply-substituted isotopologues. *Earth Planet Sci Lett* 262(3-4):309–327.
34. Eiler JM, Schauble E (2004) $^{18}O^{13}C^{16}O$ in Earth's atmosphere. *Geochim Cosmochim Acta* 68(23):4767–4777.
35. Ghosh P, Garzione CN, Eiler JM (2006) Rapid uplift of the altiplano revealed through ^{13}C-^{18}O bonds in paleosol carbonates. *Science* 311(5760):511–515.
36. Came RE, et al. (2007) Coupling of surface temperatures and atmospheric CO_2 concentrations during the Palaeozoic era. *Nature* 449(7159):198–201.
37. Affek HP, Bar-Matthews M, Ayalon A, Mathews A, Eiler JM (2008) Glacial/interglacial temperature variations in Soreq cave speleothems as recorded by 'clumped isotope' thermometry. *Geochim Cosmochim Acta* 72(22):5351–5360.
38. Morrison PR, Ryser FA (1952) Weight and body temperature in mammals. *Science* 116:231–232.
39. Seebacher F, Elsey RM, Trosclair PL, III (2003) Body temperature null distributions in reptiles with nonzero heat capacity: Seasonal thermoregulation in the American alligator (*Alligator mississippiensis*). *Physiol Biochem Zool* 76(3):348–359.
40. Seebacher F (2003) Dinosaur body temperatures: The occurrence of endothermy and ectothermy. *Paleobiology* 29(1):105–122.
41. Chabreck RH, Joanen T (1979) Growth rates of american alligators in Louisiana. *Herpetologica* 35(1):51–57.
42. Hutton JM (1987) Growth and feeding ecology of the nile crocodile *Crocodylus niloticus* at Ngezi, Zimbabwe. *J Anim Ecol* 56:25–38.
43. Satchell GH (1999) Circulatory system: Distinctive attributes of the circulation of elasmobranch fish. *Sharks, skates, and rays: the biology of elasmobranch fishes*, ed WC Hamlett (Johns Hopkins Univ Press, Baltimore), 1st Ed, pp 218–237.
44. Huntington KW, et al. (2009) Methods and limitations of 'clumped' CO_2 isotope (Delta47) analysis by gas-source isotope ratio mass spectrometry. *J Mass Spectrom* 44(9):1318–1329.
45. York D (1968) Least squares fitting of a straight line with correlated errors. *Earth Planet Sci Lett* 5:320–324.
46. Vennemann TW, Hegner E, Cliff G, Benz GW (2001) Isotopic composition of recent shark teeth as a proxy for environmental conditions. *Geochim Cosmochim Acta* 65 (10):1583–1599.
47. Guo W, Mosenfelder JL, Goddard WA, III, Eiler JM (2009) Isotopic fractionations associated with phosphoric acid digestion of carbonate minerals: Insights from first-principles theoretical modeling and clumped isotope measurements. *Geochim Cosmochim Acta* 73(24):7203–7225.
48. Guo W (2008) Carbonate clumped isotope thermometry: Application to carbonaceous chondrites and effects of kinetic isotope fractionation. PhD Thesis (California Inst of Technology).
49. Tripati A, Thiagarajan N, Eiler J (2008) 'Clumped isotope' thermometery in foraminifera. *Geochim Cosmochim Acta* 72(12):A956.
50. Thiagarajan N, Guo WF, Adkins J, Eiler J (2009) Clumped isotope calibration of modern deep sea corals and implications for vital effects. *Geochim Cosmochim Acta* 73 (13):A1324.
51. Elliott JC (2002) Calcium Phosphate Biominerals. *Reviews in Mineralogy and Geochemistry. Phosphates: Geochemical, Geobiological, and Materials Importance*, eds MJ Kohn, J Rakovan, and JM Hughes (Mineralogical Society of America and Geochemical Society, Washington, DC), Vol 48, pp 427–453.
52. von Koenigswald W (1988) Paleoclimatic implication of the last glacial mammals from the northern upper Rhine plain (Translated from German). *About the paleoclimatology of the last interglacial in the northern part of the upper Rhine plain*, ed Wv Koenigswald (Akademie der Wissenschaften und der Literatur, Mainz), (Translated from German), pp 205–314.
53. von Koenigswald W (2002) *Living Ice Age* (Theiss Verlag, Stuttgart), (Translated from German), p 190.
54. Van Kolfschoten T, Laban C (1995) Pleistocene terrestrial mammal faunas from the North Sea. *Mededelingen Rijks Geologische Dienst* 52:135–151.
55. Kahlke D (2001) A sea full of bones? Pleistocene vertebrate remains from the Schelde estuary and from the North Sea bottom (Translated from German). *Natur und Museum* 131:417–432.
56. Tütken T, Vennemann TW, Pfretzschner H-U (2008) Early diagenesis of bone and tooth apatite in fluvial and marine settings: Constraints from combined oxygen isotope, nitrogen, and REE analysis. *Palaeogeogr Palaeoclimatol Palaeoecol* 266(3-4):254–268.
57. Ayliffe LK, Chivas AR, Leakey MG (1994) The retention of primary oxygen isotope compositions of fossil elephant skeletal phosphate. *Geochim Cosmochim Acta* 58:5291–5298.
58. Koch PL, Tuross N, Fogel ML (1997) The effects of sample treatment and diagenesis on the isotopic integrity of carbonate in biogenic hydroxyapatite. *J Archaeol Sci* 24 (5):417–429.
59. Hulbert RC (1988) *Cormohipparion* and *Hipparion* (Mammalia, Perissodactyla, Equidae) from the Late Neogene of Florida. *Bulletin of the Florida State Museum* 33:229–338.
60. Morgan GS (1994) Miocene and Pliocene marine mammal faunas from the Bone Valley Formation of Central Florida. *Contributions in Marine Mammal Paleontology Honoring Frank C. Whitmore, Jr*, eds A Berta and TA Deméré (San Diego Natural History Society, San Diego), pp 239–268.
61. Kohn MJ, Law JM (2006) Stable isotope chemistry of fossil bone as a new paleoclimate indicator. *Geochim Cosmochim Acta* 70:931–946.
62. Shields G, Stille P, Brasier MD (2000) Isotopic records across two phosphorite giant episodes compared: The Precambrian-Cambrian and the late Cretaceous-recent. *Marine Authigenesis: From Global to Microbial*, eds C Glenn, J Lucas, and L Prévot-Lucas (SEPM Special Volume, Tulsa).